The fragmentation of rockfalls and the analysis of risk

Jordi Corominas, Gerard Matas & Roger Ruiz-Carulla
Division of Geotechnical Engineering and Geosciences
Department of Civil and Environmental Engineering
Universitat Politècnica de Catalunya-BarcelonaTech, Barcelona, Spain

ABSTRACT
Fragmentation is a mechanism frequently observed in rockfalls. It generates new blocks which follow divergent trajectories, defining a cone. The quantitative analysis of risk is sensitive to the rockfall fragmentation. The simulations of the trajectories of unfragmented rock masses overestimate the kinetic energy of the blocks and their run-out while they underestimate the impact probability over the exposed elements. Accounting for fragmentation requires the redefinition of the probability of reach and refining the procedure to determine the impact probability. The results of a worked example carried out at the Monasterio de Piedra in Spain, show that fragmentation has a significant but contrasting effect in the calculation of risk. Compared to the unfragmented events, the risk due to fragmental rockfalls is reduced if the slope where blocks propagate up to the analyzed section, is both long and gentle enough. The reason is that newly generated fragments travel shorter distances with less kinetic energy. This effect vanishes for large rockfalls as the fragmentation increases the risk on the exposed elements due to the greater exposure caused by the cone of fragments. The effectiveness of protection measures for rockfalls up to medium size is improved by fragmentation but still many uncertainties remain that should be analyzed in future work.

RÉSUMÉ
La fragmentation est un mécanisme fréquemment observé dans les éboulements rocheux. Il génère de nouveaux blocs qui suivent souvent des trajectoires divergentes, définissant un cône d'éboulis. L'analyse quantitative du risque est très sensible à la fragmentation des éboulements. Les simulations des trajectoires des masses rocheuses non fragmentées surestiment l'énergie cinétique des blocs et de la distance maximale parcourue, tout en sous-estimant la probabilité d'impact avec es éléments exposés. La prise en compte de la fragmentation nécessite la redéfinition de la probabilité d'atteindre et d'affiner la procédure pour déterminer l'exposition. Les résultats d'un exemple travaillé réalisé au Monasterio de Piedra en Espagne montrent que la fragmentation a un effet significatif mais contrasté dans le calcul du risque. Comparé aux éboulements non fragmentés, le risque global dû aux fragmentés est réduit si la pente où se propagent les blocs avant d'atteindre la section analysée, est à la fois longue et douce. La raison en est que les nouveaux fragments générés parcourent des distances plus courtes, avec moins d'énergie cinétique. Cet effet disparaît pour les grands éboulements car la fragmentation augmente le risque sur les éléments exposés en raison de l'exposition plus grande causée par le cône d'éboulis. L'efficacité des mesures de protection des éboulements jusqu'à la taille moyenne est améliorée par la fragmentation, mais de nombreuses incertitudes subsistent qui devraient être analysées dans les travaux futurs.

1 INTRODUCTION

Rockfalls occur widely in mountain regions. They originate by the detachment of a rock mass from a steep slope, which experiences free fall and subsequent rebound and rolling after the impact on the ground surface (Cruden and Varnes,1996). In this paper we deal mainly with events of less than $5x10^4 m^3$. This range of volumes are characterized by the fragmentation of the falling rock mass and the presence of independent block trajectories.

The analysis of the rockfall hazard and risk requires the calculation of the probability of occurrence or frequency of the events as well as the potential trajectories and kinematic parameters of the falling rock mass. Rockfall simulations are strongly affected by the uncertainties and the stochasticity of all the processes involved (Macciotta et al. 2015; Preh et al. 2015). The quantitative analysis of risk (hereinafter QRA) is increasingly used for the analysis of rockfall hazard and risk for both land use planning and the management of infrastructures and facilities. It aims at quantifying the consequences (i.e. damages, victims) in case of an occurrence of the event and their associated probabilities. In QRA, for each potential rockfall source, risk (R) is expressed as follows (adapted from Hungr and Beckie, 1998; Agliardi et al. 2009):

$$R = \sum_{j=1}^{J} \sum_{i=1}^{I} N_i . P(X/D)_i . P(T/X)_j . V_{ij} \quad [1]$$

where:

R: risk due to the detachment from a cliff of a rock mass of volume "i" on an exposed element "j" located at a distance "x" from the source.

Ni: the annual frequency of rockfalls of volume class "i".

$P(X \mid D)_i$: the probability that the detached rock mass of the size class "i" reaches a point located at a distance "x" from the source,

$P(T \mid X)_i$: the exposure or the probability that an element "j" be in the trajectory of the rock fall at the distance "x", at the timing of the arrival of the rock blocks

V_{ij}: the vulnerability of an exposed element "j" being impacted by a block of magnitude "i"

The summation indicates that the expression of the risk is calculated for a range of rockfall volumes because each one is characterized by a probability of occurrence, run-out, and probability of impact. The consequences are therefore specific of each rockfall volume.

P (X │ D) or reach probability is usually calculated with propagation models. Hundreds or thousands of trajectories are generated. P (X │ D) is calculated as the proportion of simulated events that travel up to the reference point or section, for each rockfall magnitude.

The procedure for evaluating the exposure of elements moving along linear features has long been known. It is usually performed for infrastructures such as roads, railways and it is applicable to trails as well. Hazard and risk are calculated either for the whole length of the infrastructure or in selected sections and it is dependent on the number of moving elements and the width of the section affected by the rockfall event. For people in movement, the impact probability with a rockfall is as follows (adapted from Nicolet et al., 2016):

$$P(T/S) = \frac{f_p.(w_r+l_p)}{24.1000.v_p} \qquad [2]$$

where:

f_p: the uniform flow of persons (persons/day)
W_r: the width of the rockfall debris front (m)
l_p: the length of the trail occupied by a person (m)
v_p: is the mean velocity of the person (km/h)

2 ROCKFALL FRAGMENTATION

Despite being a process often observed in nature, fragmentation of rockfalls has received relatively little attention in the scientific literature. Numerous uncertainties affect its analysis because the variables involved such as the persistence of fissures in the detached rock mass, the relative impact angle upon the ground surface, the rock strength and the ground stiffness, cannot be determined with confidence (Wang and Tonon 2010). It has been shown that fragmentation can be characterized by power laws (Turcotte, 1986; Crosta et al. 2007). This is confirmed by the volume distributions of fragments of some rockfall events inventoried and real scale tests (Ruiz-Carulla et al., 2016; Gili et al. 2016). Taking into account all these observations we developed a rockfall fractal fragmentation model (RFFM) (Ruiz-Carulla et al. 2017), which is based on a model of Perfect (1997). In this model, a cubic block of unit length is broken into small pieces according to a power law. The input of the model is either an intact rock block or a jointed rock mass characterized by an in situ block size distribution (IBSD). The output of the model is a block size distribution of the rockfall fragments (RBSD). The RFFM can be integrated into trajectographic models like RockGIS (Matas et al. 2017), a GIS-Based lumped mass model that simulates stochastically the fragmentation of rockfalls. In RockGIS, the fragmentation initiates by the disaggregation of the detached rock mass through the pre-existing discontinuities. An energy threshold is established in order to determine whether the rock block breaks or not at each impact upon the ground surface. The distribution of the initial mass between the newly generated rock fragments is carried out stochastically, according to the selected power law. The remaining energy after the impact is distributed proportionally to the mass of each fragment and the envelope of the downslope trajectories of the rock fragments approaches a cone. The process continues iteratively until all fragments stop.

In this communication, we present the effect of the rockfall fragmentation in the results of the QRA. To this end, we have analyzed two scenarios within the premises of the Monasterio de Piedra, Spain, which is a summary of a larger recent work (Corominas et al. 2018). Although in the example the risk is quantified, the main goal is to show how the risk assessment procedure has to be adapted to take into account fragmentation and how the latter affects the results and their interpretation.

2.1 QRA of fragmental rockfalls

The QRA of the fragmental rockfalls has some specificities. The initial mass is redistributed among the new generated fragments after its breakage The consequence is that the smaller fragments travel shorter distances and mobilize less kinetic energy, thus reducing P (X │ D) and the intensity of impacts (Corominas et al. 2012). In contrast, the exposure or probability of impact on the exposed elements, P (T │ X), often increases due to the divergence of the trajectories of the fragments, which widens the length of the affected analyzed section (Corominas et al. 2012; Ruiz-Carulla et al. 2015). To the authors' knowledge, no attempt has been made so far to quantify the effect of rockfall fragmentation on the run-out, the velocity of the rock blocks, the exposure and, consequently on both the hazard and risk.

2.2 Redefinition of the risk components

The risk analysis of fragmental rockfall requires redefining the way how both the reach probability P (X │ D) and the exposure P (T │ X) are calculated. Compared to the analysis of individual rock blocks, fragmentation may produce paradoxical results in the computation of P (X │ D). The simplest way to assess the probability of reach is calculating the percentage of simulated block trajectories that cross a point or reference line (Jaboyedoff et al 2005). However, when the rock mass fragments, this count may yield probabilities >1. The reason is that fragmentation may generate a number of rock fragments reaching the reference point or section, much higher that the number of initiators. To overcome this, here, the P (X│ D) is calculated as the proportion of the simulated events that reach the point or reference section, regardless whether it consist of one fragment only, or several fragments. The number of fragments, however, is considered in the calculation of the exposure.

The probability of impact or exposure P (T │ X) has to consider both the width of the falling mass (W_r) affecting the trail section and the length (l_p) occupied by the exposed element (Nicolet et al. 2016). The probability is calculated with equation [2], which is used for a variety of hazardous processes such as mudslides, snow avalanches, or debris

flows. These type of slope movement progress downslope in the form of a continuous front, whose width is W_r.

For fragmental rockfalls this scenario is somehow different. After the impact of the falling rock mass on the ground and its fragmentation, the rock fragments follow divergent trajectories that can be simplified as forming a cone (Figure 1). In plan view, the affected area is defined by the projected cone of fragments. The width of the cone (w_{cx}) varies (e.g. increases) with the downslope travelled distance (x).

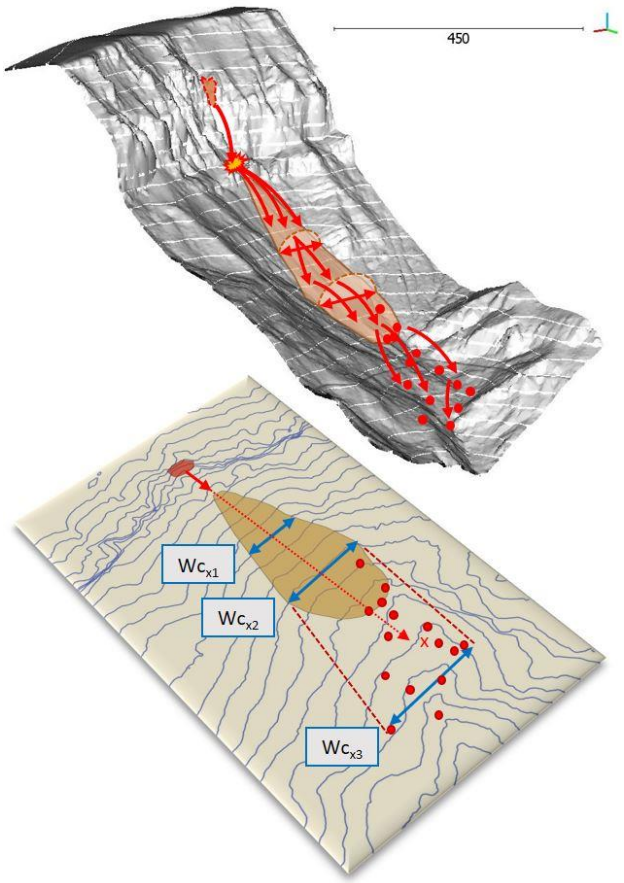

Figure 1. Sketch of a fragmental rockfall. The trajectories of the rock fragments define a cone of variable width downslope. The fragmented mass is deposited as a more or less continuous debris cover (brown polygon), as large scattered blocks (red dots), or both. The projected width (W_c) of the cone of fragments trajectories generated varies with the distance (x) to the rockfall source.

Therefore, W_{cx} is spatially distributed and must be calculated at each point or analyzed section. Large rockfall events often form a continuous debris cover of variable width (Figure 1, W_{cx1} and W_{cx2}), in this case the W_r to include in equation [2] is W_{cx}. However, in case of small to mid-size events (usually <1000m^3) or further downslope in case of larger events, the rock fragments might not completely occupy the width (W_{cx}) of the cone defined by the trajectories (W_{cx3}). In this case, the width of the rockfall (W_r) is calculated considering the fraction of the cone width actually occupied by the blocks. By increasing the size of the rockfall and the number of fragments, the proportion of the rockfall width (W_r) actually occupied by the rock blocks growths until it reaches the whole cone width (W_{cx}). To estimate W_r in equation [2], we assume that all the rock fragments reaching the analyzed section located at a distance "x" from the source, are equally sized to a modal block size (W_{mx}). The number of blocks reaching the analyzed section are counted in each simulation. Thus, the rockfall width W_r is:

$$W_r = n.\ W_{mx} \qquad [3]$$

Where "n" is the number of blocks reaching the analyzed section (at a distance "x")
W_{mx}: is the modal block width reaching the analyzed section at a distance "x" from the source

If $n.Wm \geq Wcx$, then $Wr = Wcx$

Where Wcx is the width of the cone of trajectories at a distance "x" from the source

As an example, let's assume that a 50 m^3 rockfall generates trajectories forming a 20m-wide cone at a distance of 100m from the source and the modal width W_{m100} of the fragments generated is 1 m. In case of two, ten, twenty, or forty fragments reaching the line of analysis, Wr is respectively: 0.1 W_{cx}, 0.5 W_{cx}, W_{cx}. and W_{cx}.

3 THE MONASTERIO DE PIEDRA CASE STUDY

3.1 The site

The Monasterio de Piedra is a protected natural space located in the lower reach of the River Piedra, in the central Iberian Range, NE Spain. The geological setting corresponds to a series of Mesozoic limestones, Miocene detrital formations and Quaternary tufa. The River Piedra incised and down cut the carbonate rock during the Quaternary, forming a number of small gorges and canyons in which thick Pleistocene and Holocene tufa deposits were deposited (Osácar et al. 2013). One of these gorges extends around the Lago del Espejo (Mirror lake), whose 100m-high cliffs are composed of a sequence of dolostones and limestones of Upper Cretaceous age. At the base of the cliffs predominate finely stratified limestone (30 to 50 cm-thick layers) while in the upper part the strata are massive white limestones. In addition to the stratification, which displays different dip angle at both sides of the lake, the rock mass is crossed by two main orthogonal joint sets. Dissolution processes left karstic features easily identifiable in the outcrops.

On February 17th, 2017 a rock mass of about 800 m^3 detached from the cliff above the Lago del Espejo (Figure 2). The mass fell from a 60m high vertical wall and fragmented upon the impact with the ground. The debris extended downslope to the lake, burying a section of the visitors trail. Several modules of the 1500 kJ rated rockfall barrier located just below the cliff were destroyed. A previous rockfall event of about 600m^3 occurred in October 1986 and generated debris over approximately 500m^2. Its source is located close to the 2017 event.

Figure 2. Partial view of the cliffs around the Lago del Espejo in the Monasterio de Piedra, the rockfall event of February 2017, the flexible fences, and the visitors trail.

3.2 Scenarios of analysis

The visitors trail is threatened by rockfalls originated from the whole cliff. For the sake of brevity, we present only the QRA carried out at the trail section affected by one sector of the cliffs. In this sector, rockfalls propagate over a partially forested gentle slope, in which five flexible rockfall fences, rated to 1500kJ, were built in 2002. One of those fences was destroyed by the event of 2017. Two scenarios are therefore considered: (1) the original slope situation; (2) the slope with the 1500 kJ-capacity barriers

Risk is calculated assuming a uniformly distributed flow of visitors independent of the rockfalls; all the visitors occupy the same space; the rock falls are distributed uniformly in time and space along the cliffs. Each rockfall that reaches the section of the trail is a Bernouilli trial with binary result: whether there is impact or not on the visitor (Hungr and Beckie, 1998; Agliardi et al. 2009). The source areas of the rockfalls are homogeneously distributed along the crest line of the cliff (294 sources, one every meter).

This case study analyzes the risk associated with the direct impact of rockfalls on visitors walking around the lake. Other circumstances such as people stopping for a while in the trail (for instance, working, resting, picnicking or camping) or wandering out of the trail, are beyond the scope of this analysis. In what follows, we present how the different components of equation [1] are determined.

3.3 Frequency of rockfalls Ni

The rockfall inventories are typically used to determine the frequency of the events (Bunce et al. 1997; Hungr et al. 1999; Guzetti et al. 2002; Ferlisi et al. 2012). In the Monasterio de Piedra, no complete record of rockfall events is available. We prepared the magnitude-frequency relation of rockfall events at the site, using two sources: (i) the count of rock blocks intercepted by the barriers installed in 2002, and (ii) the inventory of three large events (>400 m^3), two historical (1986 and 2017) and the third of unknown age.

A total of 209 rock blocks were measured in four barriers. This value is only an approximate estimation of the frequency because a small percentage of blocks did not reach the fences while some of the blocks retained could be part of the same event, thus underestimating its size. The volume distribution of the blocks covers three orders of magnitude and fits well to a power law. The relation has been extrapolated to the whole cliff length around the Lago del Espejo and the three large rockfalls inventoried were also included. The extrapolated frequency and the volumetric distribution of the events (arranged in bins) is presented in Table 1. The extrapolated frequency relation yields an accumulated volume of rock fall debris of about 4200 m^3 in 1000 years. Considering the exposed surface of all cliffs around the Lago del Espejo, which is 57600 m^2 (921 m in length and 60 m in height), it yields a denudation rate of the cliffs of 76 mm/ka. This rate is of the same order of magnitude as the observed in the same regional climatic context (Gutiérrez and Sesé 2001).

Table 1. Frequency of rockfall events obtained

Volume class (m^3)	Events/yr	Cumulative volume (m^3) per ka
≤ 0.005	45.1463	226
0.005< x ≤ 0,05	5.9514	523
0,05< x ≤0,5	0.7846	916
0,5 < x ≤5	0.1034	1433
5 < x ≤50	0.0136	2114
50 < x ≤500	0.0018	3013
500 < x	0.0002	4198

3.4 Reach Probability

The P (X | D) is calculated with the RockGIS code. The parameters of the model were calibrated using the rockfall event of February 2017, the location of a few blocks (volume ranging between 0.5 and 5m^3) removed from the cliff during scaling works carried out in March 2015, and the blocks retained at the rockfall barriers. The fragmentation law was calibrated with the 2017 event, using the in-situ block size distribution (IBSD) estimated at the rockfall source and measurement of the rockfall blocks size distribution (RBSD), following the approach described in Ruiz-Carulla et al. (2015). The spatial distribution of rock fragments and the run-out distances were checked using the procedure described in Matas et al. (2017).

Each source releases 100 rock masses than remain intact along the path and 10 rock masses that are fragmented, totaling 29,400 and 2,940 simulations respectively. The results are summarized in Table 2. It is important to notice that the counts correspond to the simulations that reach the trail regardless of the height of the bounce. This table shows that runout is strongly affected by both the size of the event and fragmentation. Only 12% of the modelled smallest rockfalls (<0.05m^3) reach the trail section compared to the 87% for the largest events (>500m3). For fragmental rockfalls, reaching the trail means that at least one block fragment has arrived to the trail section. The results indicate that fragmentation may strongly affect propagation if the slope is both gentle and long enough. None of the simulated rockfall events < 0.5m^3 is able to reach trail section. However, the influence of fragmentation on the reduction of the runout vanishes progressively with the increase of the rockfall size. Thus, for rockfall volumes larger than 50 m^3, the runout reduction is barely perceptible.

Table 2. Proportion of rockfall trajectories P(X|D) reaching the trail section for both unfragmented (U) and fragmented (F) rockfalls

Rockfall volume	Natural State		Flexible fences	
	U	F	U	F
<0,05	0.1194	0	0.0220	0
0,05 < x <0,5	0.3280	0	0.0647	0
0,5 < x <5	0.5896	0.0425	0.1455	0.0124
5 < x <50	0.7647	0.2327	0.7361	0.1310
50 < x <500	0.8320	0.6309	0.8312	0.5135
>500	0.8735	0,7996	0.8736	0.7574

RockGIS also counts the number of blocks reaching the section. This information is used to calculate the exposure as shown in the following chapter.

3.5 Exposure P(T | X)

The probability of the rockfall hitting visitors at a distance "x" from the source, P (T | X), takes into account two components: the probability that the person is placed within the rockfall trajectory at the moment of its occurrence and the width of the trail section intersected by the cone of rock fragments (W_r) (equation [2]). In the simulation of intact rock fall masses, W_r is the width of the fallen rock block assuming a cubic shape (table 3). For fragmental rockfalls, W_r is the fraction of the cone of debris width W_{cx} actually occupied by the rock fragments, which will be calculated with the information provided by the RockGIS code

Table 3. W_{cx} (m) values for different fragmental rockfall volumes, calculated with the RockGIS code

Volume class (m^3)	Unfragmented rockfalls	Fragmental rockfalls
x ≤ 0,05	0.2	None reaching
0,05< x ≤0,5	0.8	None reaching
0,5 < x ≤5	1.5	17.5
5 < x ≤50	3.5	20
50 < x ≤500	8	40
500 < x	10	55

The modal size and number "n" of fragments reaching the analyzed section provided by RockGIS code are included in equation [3] to calculate W_r. The procedure is summarized in Table 4, in which the block fragments have a modal with (W_{mx}) of 1 m and the width of the cone of fragments at its intersections with trail is W_{cx}=5m. Only 21% of the trajectories (reach probability=1-0.79) of the simulated fragmental rockfall events, reach the trail. This percentage is split considering the number of fragments that reach the trail in each simulation. Thus, the trail is intersected by 1, 2, 3, 4 and ≥ 5 rock fragments in 6.5%, 2%, 1%, 1% and 10.5% of the simulated trajectories, respectively.

Table 4. Example of calculation of Value of W_r (m) and its associated probability, using equation [3]. See text for details

% of simulated trajectories	# of blocks reaching the trail	P(X | D)	Fraction W_{cx}	w_r (m)
79	none	0	0	0
6.5	1	0.065	0.2	1
2	2	0.02	0.4	2
1	3	0.01	0.6	3
1	4	0.01	0.8	4
10.5	≥5	0.105	1	5

This procedure for estimating W_r in fragmental rockfall events must be repeated for each rockfall size and for each analyzed trail section.

The exposure, P (T | X) also requires considering the flow of visitors (fp). During the last 16 years, the Monasterio de Piedra natural site has received an average number of 250,040 visitors per year (696 ≈ 700 visitors/day). Different vulnerability values are heuristically assigned based on the size of the rock block and the number of persons in the group (Table 5).

4 RESULTS

The results are summarized in table 5. The two scenarios are discussed. Scenario 1 corresponds to the initial

situation, without the presence of flexible rockfall protection fences, for both unfragmented and fragmental rockfalls.

Some contrasting results of the rockfall fragmentation must be highlighted. On one side, fragmentation reduces the risk totally for rockfall volumes of less than 0.5m^3. This is because fragmentation prevents the rock fragments from reaching the trail section that is, P(X:D)=0. On the opposite side, for rockfall volumes larger than 50m^3, fragmentation raises the risk to the visitors. The reason is that the generation of the cone of fragments substantially increases P(T:X), particularly for large rockfall events whose fragments virtually occupy the whole W_{cx}. In contrast, for rockfall volumes ranging between 0.5 and 50m^3, the increased exposure is compensated by the reduction of the run-out. These effects have a direct consequence on the overall risk value as most of the risk originates from the high-frequency small-magnitude rockfall events, whose run-out is strongly affected by the fragmentation. The annual probability of loss of life for individual visitors is reduced from $1.2 \cdot 10^{-2}$ to $3.5 \cdot 10^{-4}$, which is almost two orders of magnitude.

Table 5. Individual risk (annual probability of loss of life) for intact and fragmental rockfalls considering initial situation (top) and the presence of flexible rockfall protection fences (bottom).

Initial			Unfragmented rockfalls			Fragmental rockfalls		
M_i (m^3)	Ni	V	P(X:D)	P(T:X)	Risk	P(X:D)	P(T:X)	Risk
≤ 0,05	16.32	0.5	0.119	0.010	9.9×10^{-3}	0.000	0.000	0.000
0,05 a ≤0,5	0.25	0.9	0.328	0.019	1.4×10^{-3}	0.000	0.000	0.000
0,5 a ≤5	3.3×10^{-2}	1.0	0.590	0.022	4.3×10^{-4}	0.042	0.034	4.7×10^{-5}
5 a ≤50	4.3×10^{-3}	1.0	0.765	0.066	2.2×10^{-4}	0.233	0.120	1.2×10^{-4}
50 a ≤500	5.7×10^{-4}	1.0	0.832	0.124	5.9×10^{-5}	0.631	0.374	1.4×10^{-4}
> 500	8.0×10^{-5}	1.0	0.873	0.153	1.0×10^{-5}	0.800	0.678	4.2×10^{-5}
Annual probability of loss of life					**0.012**			**3.5×10^{-4}**
Fences	Ni	V	P(X:D)	P(T:X)	Risk	P(X:D)	P(T:X)	Risk
≤ 0,05	16.32	0.5	0.022	0.0102	1.8×10^{-3}	0.000	0.000	0.000
0,05 a ≤0,5	0.25	0.9	0.065	0.0189	2.8×10^{-4}	0.000	0.000	0.000
0,5 a ≤5	3.3×10^{-2}	1.0	0.145	0.0219	1.1×10^{-4}	0.012	0.037	1.5×10^{-5}
5 a ≤50	4.3×10^{-3}	1.0	0.736	0.0656	2.1×10^{-4}	0.131	0.122	6.9×10^{-5}
50 a ≤500	5.7×10^{-4}	1.0	0.831	0.1239	5.9×10^{-5}	0.513	0.359	1.1×10^{-4}
> 500	8.0×10^{-5}	1.0	0.874	0.1531	1.0×10^{-5}	0.757	0.650	3.8×10^{-5}
Annual probability of loss of life					**2.5×10^{-3}**			**2.3×10^{-4}**

Scenario 2 considers the presence of flexible rockfall protection fences and allows for assessment of their performance in terms of their spatial arrangement and their efficiency to cope with the fragmental rockfalls.

In this scenario, the effects observed in the natural conditions, such as the runout reduction and the increase of exposure are found here as well. However, the efficacy of the flexible rockfall fences in halting the falling blocks and the subsequent risk reduction is better observed in the analysis of unfragmented rockfalls. There is a reduction of 80% of the annual risk for visitors. Most of the reduction is due to the trapping of small-size rockfall events. The reduction of risk for fragmental rockfall is less significant. The annual risk is reduced by only 35%. The reason is that most of the mid and large-size fragmental rockfalls cannot be stopped by the fences. There exist however an additional cause for this particular example. The probability of reach P(X:D) for fragmental rockfalls in the volume range of 0.5 to 5m^3, has been reduced from 0.04 to 0.01. This contrasts with the significant reduction observed for the non-fragmented events which is from 0.59 to 0.15. This is because a small percentage of modelled trajectories are not intercepted by the fences while some rebounds are higher than the height of the fences. This percentage cannot be reduced unless further protection works are carried out.

A significant percentage (over 50%) of the large rockfalls for both unfragmented and fragmental rockfalls reach the trail. The existing protection fences are not capable to stop the rock blocks. It is worth noticing however, that for the range of fragmental rockfall volumes between 5 and 50m^3, the reach probability is reduced up to 0.13.

5 DISCUSSION

Rockfall simulation is highly sensitive to the quality of the input data. Despite using a high-resolution DEM (0.2x0.2m), several sources of uncertainty remain in all the steps followed. Because of this, the example we provide is not aimed at yielding a precise value of risk but instead at highlighting the effect of fragmentation in the value of risk and in the interpretation of the results.

The first source of uncertainty is the frequency-magnitude relation, which has been prepared using a 15-yr record of rock blocks trapped in the existing fences. It is assumed that each block corresponds to one independent event obviating the fact that several of the retained blocks might be fragments belonging to the same rockfall event. This assumption underestimates the magnitude of the events (all the blocks trapped are <1m^3). Conversely, rock blocks located upslope of the flexible fences were not counted because their age cannot be constrained, which in turn underestimates their frequency. At the other end, three large rockfall events (>500m^3) are constrained by the minimum age of the gorge. Another source of uncertainty

are the rockfall release points. All the detachment points are assumed homogeneously distributed along the crest line of the cliffs. Although this hypothesis fits well for large rockfall volumes, it is clearly conservative for both small and mid-size events (up to 50 m^3) since a percentage of them originate in middle and lower sectors of the cliff face and, therefore, they develop lower kinetic energies and run-out. Furthermore, despite the fact that the RockGIS model was calibrated by the rockfall event of 2017 and by the back analysis of blocks released during scaling works in 2015, the model is based on a lumped mass approach whose restrictions are already known. The roughness is included in the restitution factors and is assumed constant for the whole slope while the vegetation has not been considered. Finally, the exposure is calculated using a variable debris front width (W_r) and modal block size (W_{mx}) rather than the actual size distribution of the blocks reaching the analyzed section.

In spite of all the uncertainties and limitations of the approach, the results indicate that fragmentation strongly affects the results of the risk analysis. However, the consequences are not obvious and must be checked at each location or analyzed section. The main reason is that both the reach probability and the exposure are spatially dependent. In the analyzed section, fragmentation clearly reduces calculated risk. The length of the propagation slope facilitates the occurrence of additional impacts that, due to the smaller size of the newly generated fragments, dissipate higher energy and consequently, travel shorter distances. As the volume of the rock fall increases, so does the size of the blocks, the divergence of the trajectories (W_{cx}), and the exposure $P(T|X)$, thereby partially compensating the reduction of the run out.

The analysis of the design of the remedial measures is beyond the scope of this paper. The scenario analyzed with flexible rockfall fences considers the present conditions at the site. The simulations show that the efficacy of the fences for mid-size events increases with the fragmentation. After the impact, the velocity of the broken mass is transferred to the smaller rock fragments, whose energies are substantially reduced. In that respect, fragmentation improves the efficiency of the protection. The existing barriers intercept virtually all (98.8%) the fragments generated by the 0.5 to 5 m^3 rockfall events, and a high percentage (87%) of the fragments generated by the 5 to 50 m^3 rockfall events. The analysis also shows that a few trajectories may avoid the barriers by either passing between them or by bouncing over them. However, the interpretation of the performance of the rockfall fences must take into account the various assumptions of the analysis. First and most importantly, the analysis does not account for the multiple block impacts. Furthermore, no damage function is applied to the fences. In the simulations, all impacts with kinetic energies below 1500 kJ are trapped without affecting the future performance of the fence. This is an arguable assumption as the efficiency of the fence may decrease below the maximum impact load, while small blocks with kinetic energy lower than the design values may puncture the fence panel by a bullet effect. As consequence, our evaluation likely overestimates the efficiency of the existing barriers.

6 CONCLUSIONS

The quantitative risk analysis of fragmental rockfall has to confront a variety of challenges related to the evaluation of the occurrence probability or frequency of the events, including the runout modelling and the behavior of the falling mass. It must also account for the uncertainties due to the inherently complex physical processes involved and the stochastic variability of all the relevant parameters. To our knowledge, this is the first attempt to address the QRA of fragmental rockfalls. It is carried out with simulations using the RockGIS code that considers a fragmentation law for the falling rock masses. Despite all the limitations, the example we present highlights the relevance of the fragmentation to exposed elements and in the quantification of the risk.

One of the most important effects of fragmentation is on the rockfall runout. Fragmentation may significantly reduce the rockfall propagation if the slope is both gentle and long enough. This is clearly illustrated in the analysis of trail section in the Monasterio de Piedra. None of the rock fragments of the small size (<0.5m^3) fragmented rock masses reached the trail section. This is the reason for the substantial reduction in calculated risk (more than one order of magnitude) compared to the value of risk for intact blocks for this magnitude range. However, the favorable effect of fragmentation would vanish if rockfalls propagate along steep slopes. The blocks can hardly stop and the cone of fragments generated increase the exposure.

Fragmentation in the risk analysis forces the redefinition of the reach probability $P(X|D)$ because a paradoxical situation may appear if a number of block fragments bigger than the number of initiators attain the distance of the analyzed section. Our analysis required a new procedure to quantify the exposure. The fragmentation due to the impact of small to mid-size rock masses (e.g. <100m^3) on the ground, generates trajectories that create a cone of fragments whose projected width on the ground surface determines the length of the trail section affected by the arrival of rock fragments (W_{cx}). The procedure followed includes the calculation of the number of fragments that reach the section and the proportion that they really occupy of the debris front width (W_r). An important effect of fragmentation is that the exposure P(T:X) is spatially dependent, as shown by the variability of the cone of fragments.

In the worked example, for rockfall events larger than 50 m^3, fragmentation notably increases the impact probability, due to the generation of the cone of fragments. This increase is counterbalanced by the reduction of the runout. The results show that the value of risk associated to both unfragmented and fragmental rockfalls is similar but the contribution of the risk components is different. This fact has to be taken into account in order to avoid misleading conclusions.

The performance of the existing flexible fences has been analyzed as well. The efficacy of rockfall fences for rockfall events up to 50m^3 increases with the fragmentation. This opens the possibility of using this type of protections to manage the risk. However, additional work is needed on the performance of these structures before

the efficiency and the residual risk could be evaluated reliably.

The analysis of fragmentation is not straightforward. It requires the availability of a diversity of input data and working with high-resolution DEM. The use of the RockGIS propagation model entails the multiparametric calibration and validation.

7 ACKNOWLEDGEMENTS

This work has been carried out with the support of the fellowship to the last two authors and within the framework of the research project Rockmodels financed by the Spanish Ministry of Economy and Competitiveness and the European Regional Development's funds (FEDER), (BIA2016- 75668-P, AEI/FEDER, UE) and by the grants to the second and third authors (BES-2014-069795 and FPU13/04252, respectively). We also appreciate all the facilities provided by Monasterio de Piedra S.A. to carry out this work.

8 REFERENCES

Agliardi, F. Crosta, G.B. and Frattini, P. 2009. Integrating rockfall risk assessment and countermeasure design by 3D modelling techniques. *Nat Hazards Earth Syst Sci* 9:1059–1073

Bunce, C.M. Cruden, D.M. and Morgenstern, N.R. 1997. Assessment of the hazard from rock fall on a highway, Can. Geotech. J 34: 344–356

Corominas, J., Mavrouli, O., Santana, D., Moya, J. 2012. Simplified approach for obtaining the block volume distribution of fragmental rockfalls. XI International Symposium on Landslides. Banff, Canada. CRC Press. Taylor & Francis Group, 2013, p. 1159-1164

Corominas, J., Matas, G., Ruiz-Carulla, R. 2018. (under review). Quantitative Analysis of Risk due to Fragmental Rockfalls. Submitted to Landslides

Crosta, G.B. Frattini, P. and Fusi, N. 2007. Fragmentation in the Val Pola rock avalanche, Italian Alps. Journal of Geophysical Res., 112, F01006,

Cruden, D.M. and Varnes, D.J. 1996. Landslide types and processes. In A. K. Turner and R. L. Schuster, eds. *Landslides: Investigation and Mitigation*. National Research Council, Transportation Research Board, Special Report 247: 36-75

Ferlisi, S. Cascini, L. Corominas, J. and Matano, F. 2012. Rockfall risk assessment to persons travelling in vehicles along a road: the case study of the Amalfi coastal road (southern Italy). Nat Hazards 62:691–721

Gili ,J.A. Ruiz-Carulla, R. Matas, G. Corominas, J. Lantada, N. Núñez, M.A. Mavrouli, O. Buil, F. Moya, J. Prades, A. and Moreno, S. 2016. Experimental study on rockfall fragmentation: in situ test design and firsts results. In: Aversa S, Cascini L, Picarelli L, Scavia C (ed) *Landslides and engineered slopes*, 2: 983-990.

Gutierrez Elorza, M. and Sesé Martínez, V.H. 2001. Multiple talus flatirons, variations of scarp retreat rates and the evolution of slopes in Almazán Basin (semi-arid central Spain). Geomorphology 38: 19–29.

Guzzetti, F. Reichenbach, P. and Wieczorek, G.F. 2003. Rockfall hazard and risk assessment in the Yosemite Valley. California, USA Natural Hazards and Earth System Sciences 3: 491-503

Hungr, O. and Beckie, R.D. 1998. Assessment of the hazard from rock fall on a highway: Discussion, Can. Geotech. J., 35: 409

Hungr, O. Evans, S.G. and Hazzard, J. 1999. Magnitude and frequency of rock falls and rock slides along the main transportation corridors of southwestern British Columbia. Canadian Geotechnical Journal, 36: 224-238

Jaboyedoff, M. Dudt, J.P. and Labiouse, V. 2005. An attempt to refine rockfall hazard zoning based on the kinetic energy, frequency and fragmentation degree, Nat. Hazards Earth Syst. Sci., 5, 621–632

Macciotta, R. Martin, C.D. and Cruden, D.M. 2015. Probabilistic estimation of rockfall height and kinetic energy based on a three-dimensional trajectory model and Monte Carlo simulation. *Landslides,* 15: 757-772.

Matas, G. Lantada, N. Corominas, J. Gili, J.A. Ruiz-Carulla, R. and Prades, A. 2017. RockGIS: a GIS-based model for the analysis of fragmentation in rockfalls. Landslides, 14: 1565–1578

Nicolet, P. Jaboyedoff, M. Cloutier, C. Crosta, G.B. and Lévy, S. 2016. Brief Communication: On direct impact probability of landslides on vehicles. Nat Hazards and Earth System Sciences, 16: 995-1004

Perfect, E. 1997. Fractal models for the fragmentation of rocks and soils: a review. Eng Geology, 48: 185-198

Preh, A. Mitchell, A. Hungr, O. and Kolenprat, B. 2015. Stochastic analysis of rockfall dynamics in quarry slopes. *Int J Rock Mech Min Sciences,* 80: 57-66.

Ruiz-Carulla, R. Corominas, J. and Mavrouli, O. 2016. Comparison of block size distribution in rockfalls. In: Aversa S, Cascini L, Picarelli L, Scavia C (eds) Landslides and engineered slopes 3: 1767-1774

Ruiz-Carulla, R. Corominas, J. and Mavrouli, O. 2017. A fractal fragmentation model for rockfalls. Landslides 14: 875-889

Sancho, C. Arenas, C. Pardo, G. Vázquez, M. Hellstrom, J. Ortiz, J.E. Torres, T. Rhodes, E. Osácar, M.C. and Auqué, L. 2010. Ensayo cronológio de las tobas cuaternarias del río Piedra (Cordillera Ibérica). Geogaceta 48: 31-34

Turcotte, D.L. 1986. Fractals and fragmentation. Journal of Geophysical Research. Solid earth 91: 1921-1926.

Wang, Y. and Tonon, F. 2011. Discrete element modeling of rock fragmentation upon impact in rock fall analysis. Rock Mech Rock Eng, 44:23–35